CONF-881009--1

CONF-881009--1

TI88 013247

Corrosion and Mass Transfer of Ferrous Alloys in Pb-17 at. % Li*

P. F. TORTORELLI (Oak Ridge National Laboratory, USA)

Abstract

Long term exposures of type 316 stainless and Fe-12Cr-1MoVW steels to thermally convective Pb-17 at. % Li demonstrated the aggressiveness of this environment, the greater corrosion susceptibility of the austenitic stainless steel, the constancy of the Fe-12Cr surface composition, and the applicability of a surface destabilization model. Cold work affected the penetration of type 316 stainless steel. Deposition in the type 316 stainless steel system appeared to be influenced by the effectiveness of nucleation and/or adhesion of deposits. In the Fe-12Cr-1MoVW steel loop, solubility-driven reactions appeared to be the most important process in deposition.

I. Introduction

The use of molten Pb-17 at. % Li as the tritium breeding fluid in fusion reactors requires detailed understanding of the corrosion of containment materials. Previous work (for example, refs. 1-7) has focused on dissolution behavior and showed that this liquid metal is quite aggressive toward ferrous alloys, particularly austenitic stainless steels. This paper reports and analyzes weight change and microstructural data for type 316 stainless and Fe-12Cr-1MoVW steels exposed to thermally convective Pb-17 at. % Li (in separate loops) for up to 10,000 h at a maximum temperature of 500°C.

II. Experimental Procedures

The experimental results were obtained by use of two thermal convection loops (TCLs) of a type described previously.[3] In one loop, type 316 stainless steels coupons were contained in type 316 stainless steel tubing that previously had circulated lithium for over 10,000 h. The second TCL contained Fe-12Cr-1MoVW ferritic steel specimens and was made from modified Fe-9Cr-1Mo steel. It had not seen prior service. Both loops circulated Pb-17 at. % Li at a maximum temperature of 500°C. The temperature differentials were 150°C in the case of the ferritic steel and 100°C for the austenitic steel loop. At all times during the exposures, four specimens were grouped at the hottest location in each loop and these specimens were selectively removed and replaced at various times. This resulted in 500°C data for cumulative exposures up to just over 10,000 h. The remainder of the specimens located around each loop were not changed out and provided 10,000 h exposure data on removal at the end of the experiments.

Low temperature molten lithium was used to remove residual lead-lithium from exposed specimens. This method was effective, but, as discussed in detail previously,[3] it can sometimes lead to partial or complete detachment of the corrosion layer on type 316 stainless steel. If a specimen cleaned in this way was again exposed, corrosion would be greater than if

*Research sponsored by the Office of Fusion Energy, U.S. Department of Energy under contract DE-AC05-84OR21400 with the Martin Marietta Energy Systems, Inc.

DISCLAIMER

the layer had not been disturbed.[3,5] Therefore, the weight change data reported below represent measurements from individual coupons, which were cleaned in the standard manner after loop exposure and not re-exposed.

The composition of the annealed and as-rolled electropolished type 316 stainless steel specimens used in this study was Fe-17Cr-12Ni-2Mo-2Mn-2Si-0.08C (wt %). The Fe-12Cr-1MoVW steel consisted of Fe-12Cr-1Mo-0.5Ni-0.6Mn-0.4W-0.3V-0.2Si-0.2C (wt %). These latter specimens were normalized and tempered (0.5 h at 1050°C, 2.5 h at 780°C, in flowing argon) and mechanically polished prior to exposure to the lead-lithium.

III. Results

Relatively large weight losses were measured for specimens held in the hottest zone of both loops. Weight loss versus exposure time curves for type 316 stainless and Fe-12Cr-1MoVW steels at 500°C are shown in Fig. 1, which also includes some previously reported data.[3] For a given exposure time, the plot of specimen weight change versus position in the loop yields an approximate mass transfer profile. Such measurements after more than 10,000 h exposure of the two steels in the thermally convective Pb-17 at. % Li are shown in Fig. 2. (The weight losses and gains do not balance because coupons are not positioned everywhere in the loops.)

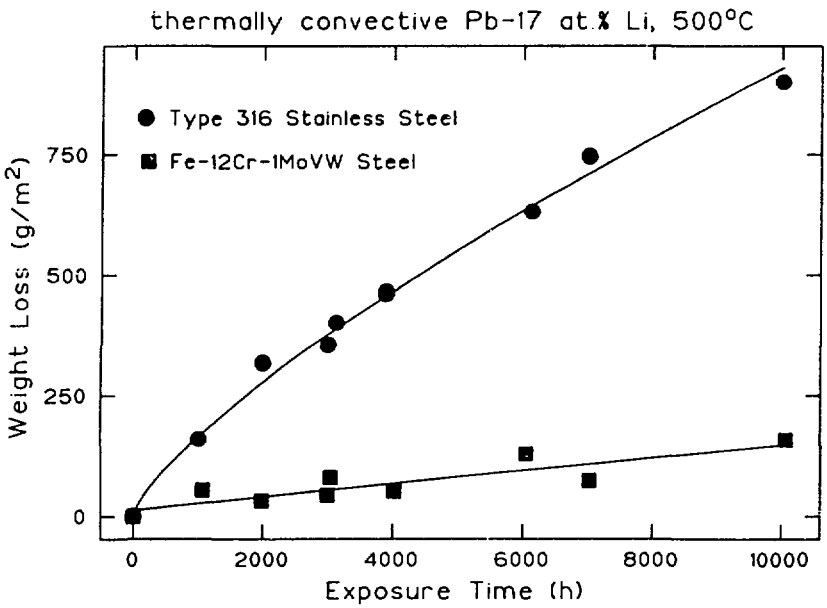

Fig. 1. Weight loss versus exposure time for type 316 stainless steel and Fe-12Cr-1MoVW steel exposed to thermally convective Pb-17 at. % Li at 500°C.

After exposure, the surfaces of the type 316 stainless steel were much rougher than that of similarly exposed Fe-Cr ferritic steel. Such differences in corrosion-induced morphologies have been noted previously[3,4] and are quite striking when such specimens are examined in cross section, Fig. 3. Whereas the Fe-Cr steel tended to corrode uniformly throughout the 10,000 h of exposure, the Fe-Ni-Cr austenitic stainless steel suffered severe localized corrosion, resulting in deep penetrations into the specimens. Furthermore, as illustrated in Fig. 4, the depth and directionality of penetration were found to depend on the particular coupon face exposed to the Pb-17 at. % Li. The corrosion zone was thicker on the "short"

sides than on the longer faces. Furthermore, the main branch penetrations appear perpendicular to the original surface on the "short" side and parallel to the "long" sides.

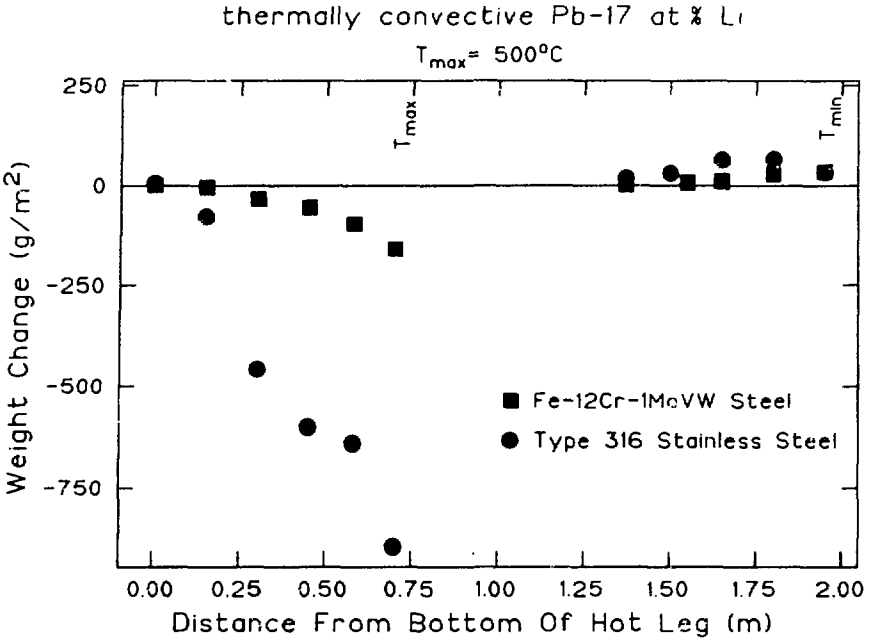

Fig. 2. Weight change versus loop position in thermally convective Pb-17 at. % Li at a maximum loop temperature of 500°C for type 316 stainless steel exposed for 10,008 h and Fe-12Cr-1MoVW steel exposed for 10,076 h.

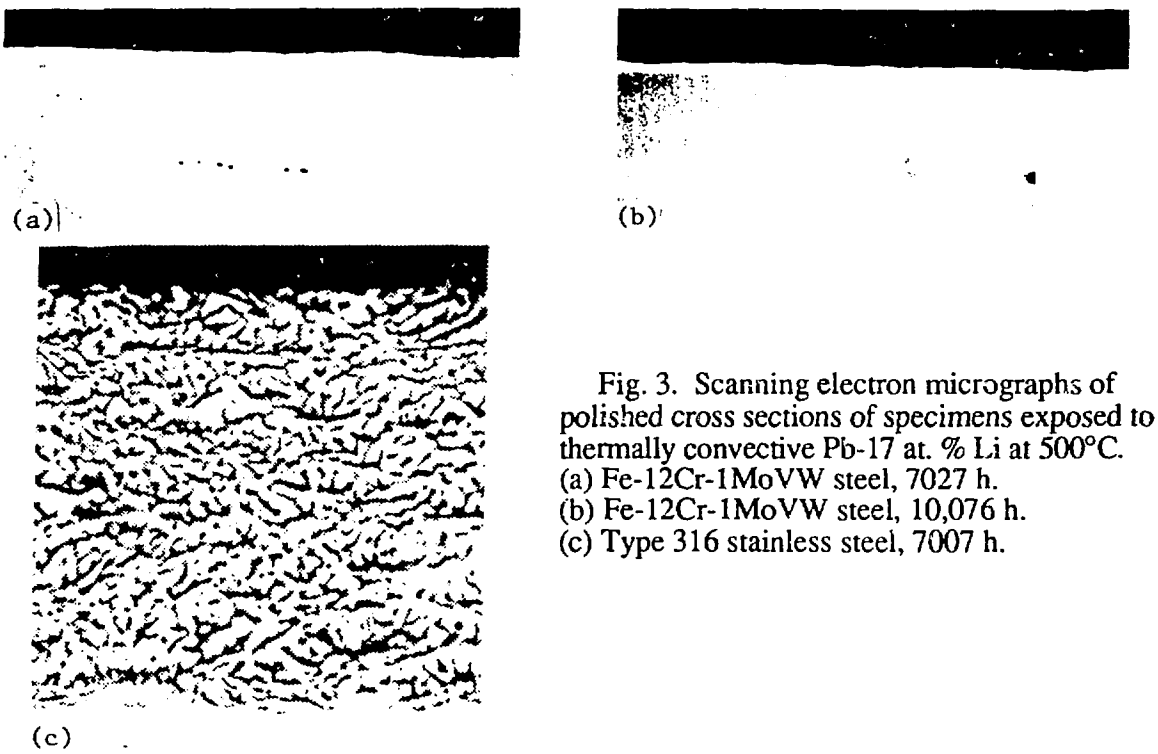

Fig. 3. Scanning electron micrographs of polished cross sections of specimens exposed to thermally convective Pb-17 at. % Li at 500°C.
(a) Fe-12Cr-1MoVW steel, 7027 h.
(b) Fe-12Cr-1MoVW steel, 10,076 h.
(c) Type 316 stainless steel, 7007 h.

Fig. 4. Scanning electron micrograph of polished cross sections of type 316 stainless steel exposed to thermally convective Pb-17 at. % Li at 500°C for 7007 h. (a) Long face of coupon. (b) Short face.

Energy dispersive x-ray analysis (EDX) of exposed surfaces revealed a substantial change in the surface composition of the type 316 stainless steel, but there was very little difference between the unexposed and exposed surface compositions of the Fe-12Cr-1MoVW steel. For example, after 7007 h at 500°C, the surface composition of the exposed type 316 stainless steel was Fe-8Cr-3Ni (wt %), while that of the Fe-12Cr-1MoVW steel was Fe-12Cr after 7027 and 10,076 h of exposure to Pb-17 at. % Li. EDX data obtained from polished cross sections of type 316 stainless steel showed that the (depleted) concentrations of nickel and chromium were constant throughout the extended depth of the penetrated regions and a sharp transition to the starting composition was found at the interface between the penetration front and the undisturbed material.

In nonisothermal liquid metal systems, the deposition of dissolved species in the cold zone can be as important as the dissolution processes in the hotter parts of the circuit. Therefore, the exposed surfaces and polished cross sections of the cold leg coupons from the type 316 stainless steel loop experiment were analyzed by scanning electron microscopy and associated EDX. Representative regions from selected specimens are shown in Fig. 5. On any one particular specimen, variations in deposit density were noted and, on some coupons, there were rather large areas free of deposits (possibly removed during handling and/or cleaning). The compositions of mass transfer deposits on each type 316 stainless steel cold leg specimen were determined by EDX. Table 2 lists the average elemental concentrations of the deposits viewed either looking directly down on them or in cross section. A marked dependence of deposit composition on loop temperature and position was noted. At the higher temperature positions in the cold leg (460 and 445°C), the deposits were principally iron, while at lower temperatures, they were either iron-nickel or chromium-rich, thereby necessitating the reporting of two different average compositions in Table 1. At 430°C, most of the deposits were iron-nickel, while chromium-rich deposits dominated at 415°C. At the coldest loop coupon position (400°C), most deposits were chromium-rich, with a few being a mixture of these two compositions. X-ray diffraction of the surfaces containing these deposits showed only the presence of bcc and fcc structures consistent with metallic deposits of the compositions in Table 1 and the underlying austenitic stainless steel.

In contrast to the results for the type 316 stainless steel TCL, the compositions of the deposits on the ferritic steel loop specimens did not vary with position in the cold leg. EDX analysis showed almost all deposits to consist of Fe + 8-9 wt % Cr.

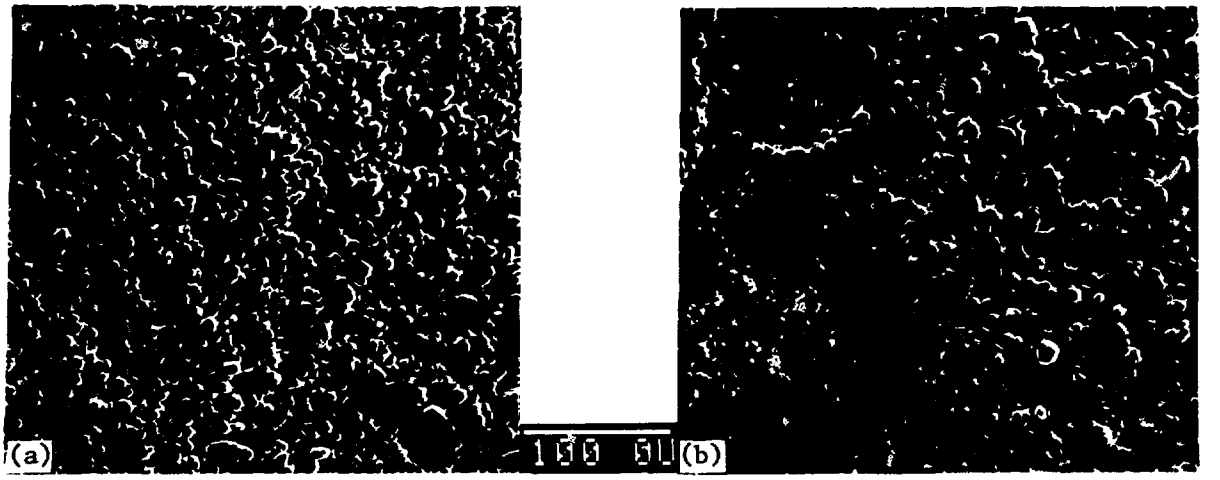

Fig. 5. Scanning electron micrographs showing the normal view of selected type 316 stainless steel specimens exposed in the cold leg of a thermal convection loop that circulated Pb-17 at. % Li at a maximum temperature of 500°C.
(a) 455°C. (b) 415°C.

Table 1. Compositions of mass transfer deposits on type 316 stainless steel coupons in cold leg of Pb-17 at. % Li thermal convection loop after 10,008 h of exposure

Cold leg temperature (°C)	Deposit concentration (wt %)[a]									
	Normal viewing					Cross section				
	Fe	Cr	Ni	Si	Mo	Fe	Cr	Ni	Si	Mo
460	90	7	3	0.4	0.4	91	5	3	0.4	0.1
445	90	7	2	0.2	0.1	90	7	3	0.4	0.0
430	51	12	36	0.3	0.1	50	12	38	0.7	0.1
	29	68	4	0.0	0.0	37	53	10	0.4	0.2
415	34	64	2	0.2	0.5	27	70	2	0.3	0.0
	45	13	41	0.4	0.7	42	14	44	0.5	0.1
400	25	70	4	0.2	0.6	27	71	1	0.4	0.1
						42	25	32	0.7	0.1

[a]Determined by energy dispersive x-ray analysis. Two average compositions given when distinct types of deposits were detected.

IV. Discussion

Comparison of the current experimental results to previous work with Pb-17 at. % Li (for example, refs. 1-7) and earlier investigations with pure lead (such as refs. 8 and 9) confirms and extends past observations, particularly with respect to the aggressiveness of this environment, the importance of preferential dissolution, and the poorer performance of the nickel-containing steel. Of more significance, the present work offers data on mass transfer deposits in these systems and some greater insight into the dissolution kinetics and the mechanism of penetration of austenitic stainless steel by lead-lithium.

A. Corrosion of hot leg specimens

The type 316 stainless steel data in Fig. 1 reflect kinetic behavior similar to that observed over a shorter period;[3] a power curve fit adequately describes the data and suggests mixed reaction rate control. The longer time data can be adequately described by linear kinetics, and the slope of a fitted straight line for times greater then 3000 h can be used to determine a "steady-state" dissolution rate. In this case, a value of 77 mg/m^2•h was obtained. This rate agrees with that derived earlier[3] from more limited data between 3000 and 6000 h: 76 mg/m^2•h. In the case of the Fe-12Cr-1MoVW steel, the weight loss data show a linear time dependence over the entire exposure range (see Fig. 1). The dissolution rate obtained from the slope is 14 mg/m^2•h, which is significantly different from that determined previously[3] from just five data points between 0 and 6000 h. In view of the penetration process for type 316 stainless steel (see Figs. 3 and 4), it must be recognized that the higher steady-state (long-term) dissolution rate of the austenitic steel relative to that of the Fe-Cr-1MoVW steel is at least partly due to the much higher specific surface area that develops on the latter steel. The 500°C dissolution rates for both steels are significantly greater than those for lithium under otherwise similar environmental conditions.[3,5] Applications of Pb-17 at. % Li must therefore be limited to lower temperatures than if pure molten lithium was being used.

While there is some scatter in the weight loss measurements (see Fig. 1), there was extremely close agreement when coupons were exposed for identical periods of time and then cleaned under exactly the same conditions. In the case of type 316 stainless steel, two specimens simultaneously exposed for 3886 h showed weight losses of 461 and 466 g/m^2. Each of two specimens of Fe-12Cr-1MoVW steel exposed for 4027 h showed weight losses of 50 g/m^2. These results indicate that, under identical exposure and handling conditions, weight loss data from lead-lithium are quite reproducible and that the observed scatter in the data probably arises from differences in the efficiency of a particular lithium rinsing procedure in removing the residual lead. However, the amount of such lead must be small since energy dispersive x-ray analysis of exposed surfaces rarely detected the presence of this element.

The striking difference in the surface recession behavior between austenitic and ferritic steels when exposed to lead-lithium can be explained using a previously-described surface destabilization model.[3] In this model, which is based on the original work of Harrison and Wagner,[10] a surface that undergoes preferential dissolution develops a very nonuniform, rugged corrosion front, while, in the absence of such selective leaching, an initially plane surface recedes uniformly. The present results confirm the applicability of such a model. The development of a very irregular solid-liquid interface on the type 316 stainless steel accompanied the preferential dissolution of nickel and chromium, while the Fe-12Cr-1MoVW steel, whose surface composition did not detectably change during the corrosion process, maintained a planar liquid-solid interface throughout the >10,000 h exposure (Fig. 3).

The surface destabilization model is also consistent with the observed morphological differences between the long and short faces of corroded type 316 stainless steel specimens. This difference in penetration morphology strongly suggests that the process leading to such irregular attack must be sensitive to the steel's microstructure. Indeed, when selected specimen cross sections were etched to reveal the grain structure, definite grain elongation parallel to the direction of main branch penetration was observed. The effect of cold work was to "bias" the penetration by the lead-lithium and can be accommodated within the surface destabilization model,[3] which requires an initial perturbation of the starting planar surface to trigger the destabilization and subsequent growth of an irregular interface. Grain boundaries or slip lines can serve as such perturbation sites.[10] Therefore, the biasing provided by the presence of slip lines and the elongation of grain boundaries in the direction of rolling can lead to the morphological differences between corrosion zones that develop on long and short faces of the same coupon. Indeed, Fauvet et al.[1] attributed their observation that cold working increased the attack of type 316L stainless steel by Pb-17 at. % Li to the presence of slip lines in the worked material. Additionally, the production of additional "nucleation" sites for penetration leads to more channels for dissolution and, therefore, larger weight losses for worked material than for annealed austenitic steel, as reported by Fauvet et al.[1] and Chopra and Smith.[4]

Surface destabilization and the observation of a microstructural dependence for the penetration of type 316 stainless steel have important implications for the measurement of corrosion losses, particularly in terms of sound metal loss and corrosion zone thickness. The comparison of such measurements from different experiments must be done with careful consideration of how specimens were prepared and analyzed. As a result of the irregular corrosion process, calculations of surface recession of solid metal cannot be obtained from the dissolution (weight loss) rate measured for the type 316 stainless steel.

As described in the Results section, both chromium and nickel are preferentially dissolved from type 316 stainless steel exposed at 500°C, while no leaching occurred from the Fe-12Cr-1MoVW steel. These results have been observed previously in nonisothermal Pb-17 at. % Li loops after shorter exposure times.[3,4] Some selective dissolution of chromium has also been seen in static Pb-17 at. % Li (ref. 2), but not to the same extent. The reason for preferential removal of chromium from the type 316 stainless steel, but not from the Fe-Cr steel, is not clear. There is some evidence that there may be an influence of other elements on the effective solubility of a particular element in lithium,[11] but the significance of such in the present case is uncertain. This depletion may be indicative of a higher activity of chromium in type 316 stainless steel than in the ferritic steel, particularly if the leaching of nickel from the austenitic steel preceded the start of chromium loss. However, the selective dissolution of chromium from type 316 stainless steel is not thought to be related to formation of a corrosion product like Li_9CrN_5 (ref. 12), which would have had to be removed during exposure or during specimen cleaning. These reactions do not occur in Pb-17 at. % Li at relevant nitrogen pressures[2,13] and the formation of such a product during lithium soaking is precluded by the low temperature of the cleaning procedure and the associated sluggish reaction kinetics. Furthermore, microprobe examination of polished cross sections of specimens from which the lead-lithium had not been removed still showed chromium depletion.[3]

The constancy of the nickel and chromium concentrations throughout the penetrated zones of type 316 stainless steel, which, after long exposures, can be greater than 80 μm in depth, can be explained in terms of the availability of the channels of liquid metal within this region. Diffusion processes in the channels, rather than solid state diffusion in the adjoining alloy matrix, will tend to control mass transport after an initial period. Such a process is consistent with the observed weight loss kinetics, which represents the integrated flux of all the elements.

Specifically, the type 316 stainless steel data of Fig. 1 can be interpreted in terms of initial parabolic behavior (required for the surface destabilization) followed by a "steady-state" regime characterized by linear kinetics , where solid state diffusion does not control the release of elements (in particular, nickel and chromium) to the liquid metal.

B. Mass transfer and deposits on cold leg specimens

The net flux, J_i, of a given element out of a specimen exposed to the molten lead-lithium can be expressed as

$$J_i = k_i (C_i^o - C_i)$$

where k_i is the overall (net) rate constant for dissolution or deposition of element i, C_i^o is the solubility of that element in the liquid metal at a particular temperature, and C_i is the actual concentration of i in the liquid. For the present purposes, C_i can be considered constant around the loop so that the variation of the solubility with temperature determines whether dissolution ($C_i^o > C_i$, $J_i > 0$) or deposition ($C_i^o < C_i$, $J_i < 0$) occurs. The positioning of coupons around the loops therefore allows measurement of mass transfer profiles for a given exposure time (see Fig. 2) and also provides information on the types of deposits that form in the cold zone (see Fig. 5 and Table 1).

Figure 2 indicates that substantial mass was transported from the hot zone during the >10,000 h exposure periods and that, despite much greater weight losses for the type 316 stainless steel, approximately the same coupon weight gains were measured in both loops. Such data may indicate that much of the deposition in the austenitic stainless steel TCL was preferentially occurring on the loop walls or in portions of the loop not containing specimens or may reflect the higher minimum loop temperature. In view of the above equation, and as discussed by Tas et al.,[6] a relatively high solubility of a particular element (Ni, for lead-lithium) may result in appreciable deposition only at a temperature below that of the nominal minimum for the loop or, at least, in an inaccessible cold part of the loop. However, in the present case, the observation of nickel-enriched deposits at intermediate temperatures in the cold zone (see Table 1) is inconsistent with a solubility-driven process. The imbalance between weight gains and losses in the type 316 stainless steel loop may be due to poor adhesion. As noted in the results section, the deposit density on the cold leg specimens in the type 316 stainless steel loop were highly variable. One reason for such variability in deposit coverage appeared to be related to the adhesion of deposits, particularly for the lower temperature coupons. Decohesion of deposits may have occurred during exposure to the liquid metal, during cooling after removal from the liquid stream, and/or during the specimen cleaning process with lithium. However, in some cases, deposits may have preferentially formed on certain areas of a specimen. The observations of small deposits in definite patterns on some of the surfaces [such as shown in Fig. 5(b)] may support such a hypothesis, particularly in view of the variability of deposit coverage from one specimen position to another and the accompanying change in deposit composition (see Table 1). The nucleation of deposits requires registry with the underlying surface and, given that the starting compositions of all the cold leg specimens were the same (type 316 stainless steel), the accommodation and sticking of deposits of differing composition may vary considerably. Similarly, variation in substrate composition may be a reason for preferential deposition on cold leg loop walls. Because, as noted above, the type 316 stainless steel TCL had been used for lithium studies before the current experiments with Pb-17 at. % Li, the composition of the cold leg wall was probably changed by prior deposition. Therefore, the loop wall could have been favored over the specimen coupons for subsequent deposit nucleation during operation with lead-lithium.

The appearance of substantial deposit-free areas on the surfaces at the two coldest loop positions in the type 316 stainless steel loop can help explain another feature of its mass transfer profile (see Fig. 2): the maximum weight gain was not at the coldest loop position, but rather at a higher temperature. Physical processes such as decohesion or lack of epitaxy could prevent thermodynamically-favored deposition, but this observation can also be explained based on the fact that, when $C_i^\circ < C$, k and $|C_i^\circ - C|$ vary in opposite directions with respect to temperature. Depending on the relative magnitude of these kinetic and thermodynamic terms, this can result in a maximum weight gain at an intermediate temperature in the cold leg.

The variation in overall deposit composition with temperature (see Table 1) can be attributed to one or more factors: temperature coefficients of elemental solubilities, differing elemental deposition kinetics and/or sticking coefficients, various chemical reactions in the liquid or at the interface, and hydrodynamics. While the present data are not sufficient to definitively rank these factors in order of importance, it is apparent that, as discussed above, the variation of deposit composition cannot strictly be explained on the basis of solubilities; the transition from iron to iron-nickel to chromium-rich deposits as the temperature decreases is not consistent with the solubilities of these elements in lead-lithium. Furthermore, the lack of any x-ray diffraction evidence of nonmetallic deposits on the cold leg specimens would seem to indicate that chemical reactions with carbon are not playing an important role in this case. The relative consistency of the deposit composition throughout the cold leg of the Fe-12Cr-1MoVW steel loop is in sharp contrast to the results for the type 316 stainless steel TCL and, with the increasing weight gains with decreasing temperature, would tend to indicate that solubility-driven deposition is the most important factor for the ferritic steel system.

V. Summary

1. Long term exposures of type 316 stainless and Fe-12Cr-1MoVW steels to thermally convective Pb-17 at. % Li confirmed the aggressiveness of this environment, the greater corrosion susceptibility of the austenitic stainless steel, the constancy of the Fe-12Cr surface composition, and the applicability of a surface destabilization model in explaining the penetration process for type 316 stainless steel over extended periods of time.

2. Microstructure had an important influence on the way type 316 stainless steel was penetrated by the lead-lithium. The effect of cold work was to bias the penetration process and was shown to be accommodated within the surface destabilization model. Such behavior has significant implications for evaluation of the corrosion phenomena.

3. The uniform depletion in nickel and chromium throughout the corrosion zone of type 316 stainless steel appeared to be a consequence of the availability of localized channels of liquid metal and the development of such was consistent with the measured weight loss kinetics.

4. Deposit composition was a function of temperature only in the type 316 stainless steel system. Deposit density in the austenitic stainless steel loop appeared to be related to the effectiveness of nucleation and/or adhesion rather than to elemental solubilities. In the Fe-12Cr-1MoVW steel loop, solubility-driven reactions appeared to be the most important process in deposition.

VI. References

1. P. Fauvet, J. Sannier, and G. Santarini, pp. 1003-09 in Proc. 13th Symp. on Fusion Technology, Vol. 2, Commission of the European Communities, Pergamon Press, 1984
2. V. Coen et al., pp. 347-354 in Proc.3rd Int'l. Conf. on Liquid Metal Engineering and Technology, Vol. 1, The British Nuclear Energy Society, 1984
3. P. F. Tortorelli and J. H. DeVan, J. Nucl. Mater. 141-143 (1986) 592-598.
4. O. K. Chopra and D. L. Smith, J. Nucl. Mater. 141-143 (1986) 566-570.
5. G. M. Gryaznov et al., Sov. At. Energy 59 (1985) 918-921.
6. H. Tas et. al., J. Nucl. Mater. 141-143 (1986) 571-578.
7. H. U. Borgstedt et al., "Corrosion Testing of Steel X 18 CrMoVNb 12 1 (1.4914) in a Pb-17Li Pumped Loop," Proceedings of 3rd International Conference on Fusion Reactor Materials, 1987, to be published in J. Nucl. Mater.
8. J. V. Cathcart and W. D. Manly, Corrosion 12 (1956) 43-47.
9. R. C. Asher, D. Davies, and S. A. Beetham, Corr. Sci. 17 (1977) 545-547.
10. J. D. Harrison and C. Wagner, Acta Metall. 7 (1959) 722-735.
11. N. M. Beskorovainyi et al.,Sov. Mater. Sci. 16 (1980) 246-250.
12. M. G. Barker et al., J. Nucl. Mater. 114 (1983) 143-149
13. W. R. Watson and R. J. Pulham, pp. 99-102 in Proc.3rd Int'l. Conf. on Liquid Metal Engineering and Technology, Vol. 3, The British Nuclear Energy Society, 1985